RECOMMENDED PROCEDURE

FOR CALCULATING WAVE DAMPING

DUE TO VEGETATION EFFECTS AND WAVE INSTABILITY

by

Robert G. Dean

Prepared For

Department of Housing and Urban Development
Washington, D. C.

Research Report CE-82-30

May 1979

DEPARTMENT OF CIVIL ENGINEERING
UNIVERSITY OF DELAWARE
NEWARK, DELAWARE
19711

TABLE OF CONTENTS

TABLE OF CONTENTS
(Continued)

RECOMMENDED PROCEDURE
FOR CALCULATING WAVE DAMPING
DUE TO VEGETATION EFFECTS AND WAVE INSTABILITY

EXECUTIVE SUMMARY

This report describes a series of wave tank tests to evaluate the decay in wave height as waves propagate through simulated vegetation. A total of 73 tests was conducted with vegetation simulated at four different densities (including no vegetation), at two different water depths and at three different wave heights per water depth.

The analysis of the wave tank test results supports two significant mechanisms of wave damping. One is related to the fluid drag forces occurring on the vegetation elements and the second is termed a "wave instability effect" and occurs due to the somewhat delicate stability of a near-breaking wave. Once the "wave instability" mechanism is initiated, wave energy dissipation will continue until the ratio of wave height to depth, H/h, is approximately 0.3, considerably smaller than the customarily accepted value of 0.78 for initiation of breaking.

This report recommends that both mechanisms of wave damping be included in the computation procedure. Where uncertainties existed in the calculation procedure, the recommended procedure was developed such that the resulting wave heights would be somewhat lower than would actually occur.

The recommended calculation procedure can be employed analytically if either the damping due to vegetation or wave instability is dominant as follows

a) Damping Due to Vegetation

$$H(x) = \frac{1}{1 + \Delta H_o x}$$

in which

H_o = the wave height at x = 0

x = coordinate in direction wave travels

$$A = \frac{C_D D}{3\pi\delta^2 h}$$

C_D = drag coefficient ($\approx$1.0)

D = diameter of equivalent vegetation element, extending over the entire water column.

δ = equivalent center-to-center spacing of the vegetation elements

h = mean water depth, accounting for effect of storm tide

b) Damping Over a Horizontal Bottom Due to Wave Instability Effect

$$H(x) = \sqrt{H_s^2 + (H_o^2 - H_s^2)e^{-Kx/h}}$$

in which

H_s = "stable" wave height taken as 0.30 of the water depth

K = wave instability coefficient determined as 0.08

c) Damping Over a Horizontal Bottom Due to Combined Effects of Vegetation and Wave Instability

In this case it is recommended that a simple numerical procedure be developed to calculate the wave height advancing in a stepwise fashion from a position of known wave height, x_j to x_{j+1}. This procedure is defined as

$$H_{j+1} = H_j - \Delta x\left[AH_j^2 + \frac{K}{2hH_j}(H_j^2 - H_s^2)\right], \quad H_j > H_s$$

$$H_{j+1} = H_j - \Delta x A H_j^2, \quad H_j < H_s$$

in which $\Delta x = x_{j+1} - x_j$ and the remaining symbols have been defined previously. The method could be extended readily to include effects of a sloping bottom or vegetation whose characteristics vary with distance.

I. INTRODUCTION

As waves propagate through vegetation, the attendant friction causes energy losses and an associated decrease in wave height. For an idealized case of tree trunks on a square spacing, δ, of diameter, D, drag coefficient, C_D, and extending over the entire water depth, h, the National Academy Study proposed the following equation for the variation of wave height, H, with distance, x

$$H(x) = \frac{H_o}{1 + AH_o x} \qquad (1)$$

in which H_o is the wave height at x = 0 and C_D is embodied in the parameter, A

$$A = \frac{C_D D}{3\pi\delta^2 h} \qquad (2)$$

This report describes a series of wave tank tests to evaluate the validity of Eq. (1) and to recommend modifications to this equation if necessary.

II. TEST FACILITIES

The tests were carried out in one of the University of Delaware wave tanks. The particular tank is 26.5 meters in length, approximately 1 meter deep and 0.61 meters wide. A piston-type wavemaker is located at one end of the wave tank; both the stroke and frequency of the wavemaker are variable providing continuous ranges of wave heights and periods. At the down-wave end of the wave tank a ramp section and plywood false bottom were constructed, the latter forming the base for the simulated forest.

The forest was represented by vertical dowels cantilevered upward from the plywood base. The dowels were 0.48 cm in diameter and tests were carried out with the following four densities: (1) full density-dowels on 5.1 cm centers; (2) half-density dowels on average 10.2 cm centers; (3) one-quarter density-dowels on average 20.3 cm centers; and (4) no dowels present. Figures 1 and 2 present respectively the profile of the false bottom used in the wave tank tests and the arrangement of the dowels for the various densities.

For a given test, waves were measured along the centerline of the wave tank at 10 cm increments using a capacitance wave gage. This resulted in 36 measurements of wave height for each test.

Some wave reflection occurred from the end of the wave tank and modified the wave height compared to that which would occur if only an incident wave were present. Figure 3 presents the measured wave height for Run F-3.. If no wave reflections or other spurious effects were present, the variation of wave height with distance would be monotonically decreasing. Successive maxima (or minima) are spaced at a distance of one-half the wavelength for wave reflection effects.

III. TEST PROGRAM

A total of 73 tests was conducted. The nominal characteristics of these runs are presented in Table I.

As noted, the wave heights were tested at near-breaking, one-half, and one-quarter of the breaking wave height. It was found to be difficult and extremely time-consuming to adjust the wavemaker stroke to just achieve breaking at the start of the "forested" area. Thus the "breaking" wave heights should be regarded as being within approximately 10-20% of the breaking heights.

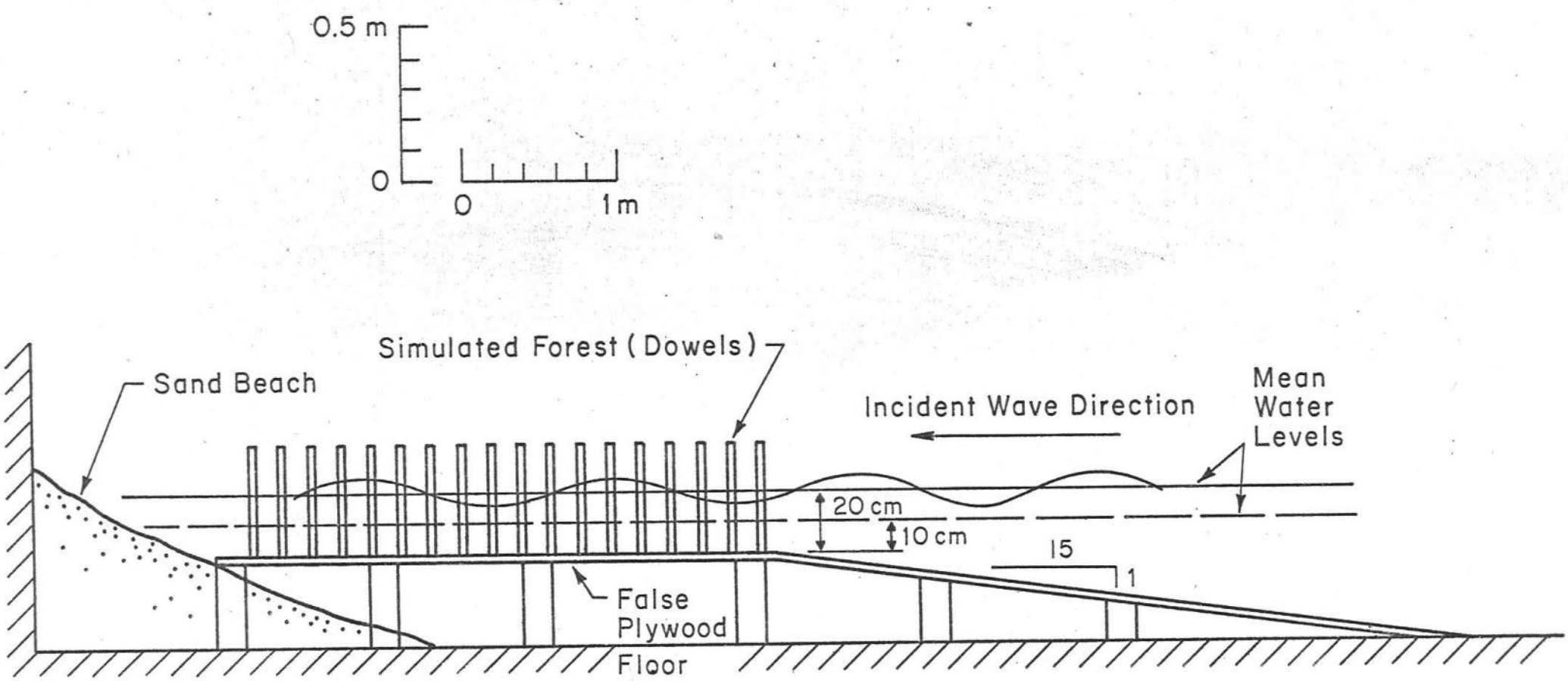

FIGURE 1. SCHEMATIC OF TEST ARRANGEMENT.

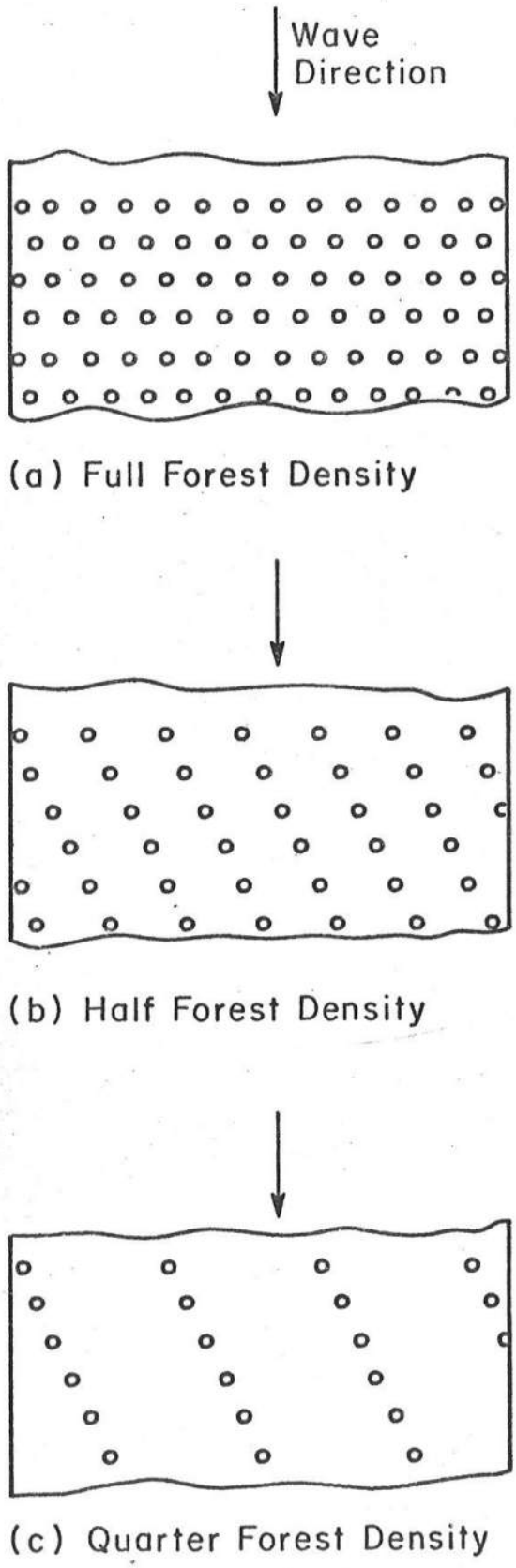

FIGURE 2. ARRAYS OF THREE FOREST DENSITIES USED IN TEST PROGRAM.

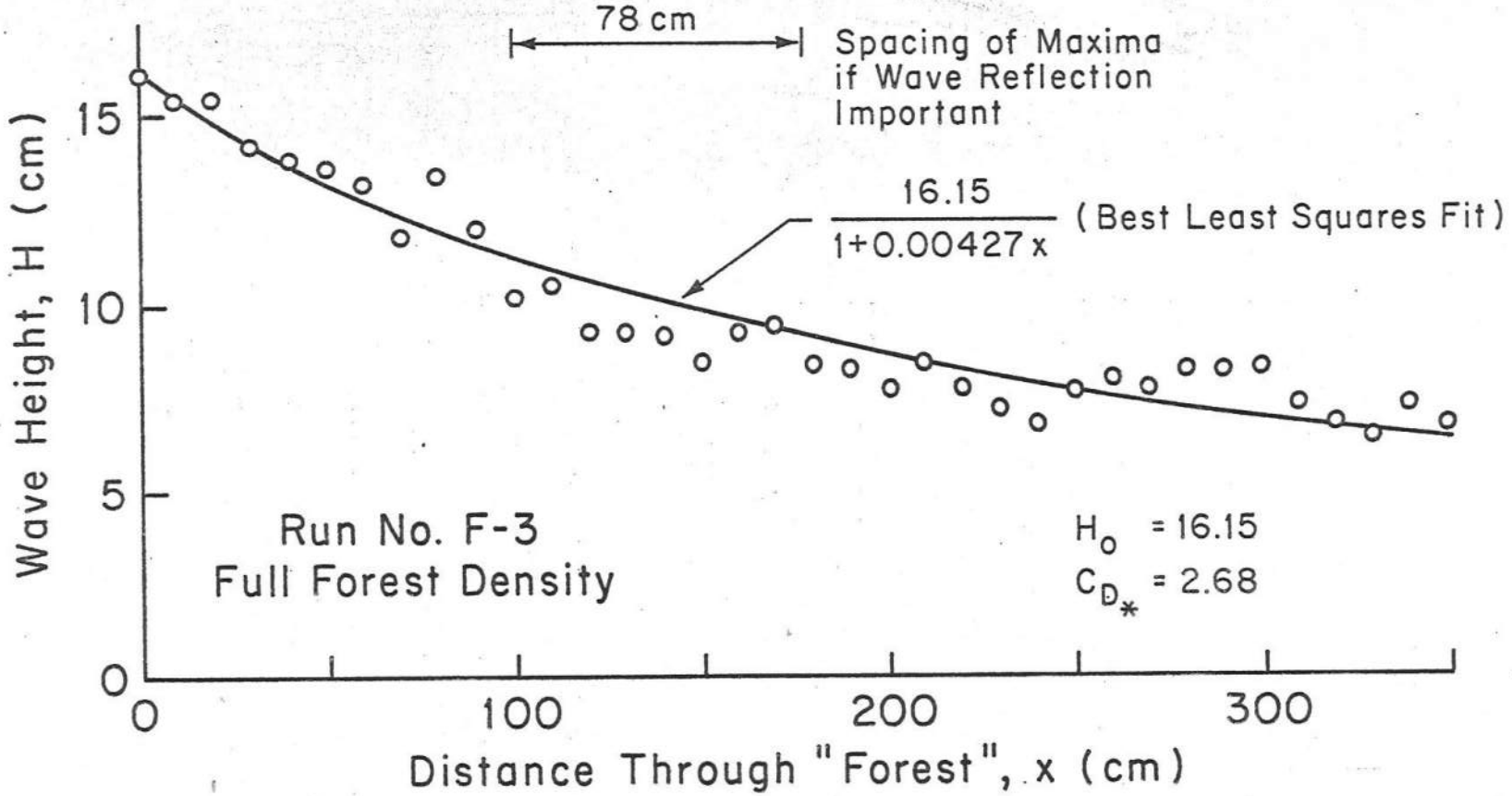

FIGURE 3. COMPARISON OF MEASURED WAVE HEIGHT VARIATION WITH BEST LEAST SQUARES FIT.

TABLE I

NOMINAL WAVE TANK TEST CONDITIONS

Density of Dowels	Average Center-to-Center Dowel Spacing	Water Depths (cm)	Nominal Wave Heights (cm)	Nominal Wave Periods (sec)	Total No. of Tests
Full	5.1 cm	10, 20	Breaking, One-Half and One-Quarter Breaking	1.0, 1.3, 1.6	19
Half	10.2 cm	"	"	"	18
Quarter	20.3 cm	"	"	"	18
None	∞	"	"	"	18

TOTAL TESTS = 73

IV. METHOD OF ANALYSIS

The data consisted of measured wave heights every 10 cm along the centerline of the 3.7 m long forested region; this resulted in 36 values of measured wave heights for each test. A method was desired to extract from these data, in a reproducible manner, a valid estimate of the drag coefficient, C_D, based on the relationship

$$H(x) = \frac{1}{1 + H_o Ax} \tag{3}$$

in which

$$A = \frac{C_D D}{3\pi\delta^2 h} \tag{4}$$

As noted previously, one of the difficulties was some degree of wave reflection from the down wave end of the tank which resulted in wave height measurements which were not quite monotonic, but varied as shown in Figure 3.

It would be possible to fit a curve "by eye" to these data of the form of Eq. (3). To ensure that a consistent and reproducible procedure was employed, a least-squares method was used in which the mean square of the deviation between the measured and predicted wave heights was minimized, i.e.

$$\underset{H_o,A}{\text{Min}} \sum_i (H_{p_i} - H_{m_i})^2 \qquad (4)$$

where H_{p_i} is given by Eq. (3).

Because H_p is nonlinear in the variables to be determined (H_o and A), an iterative least-squares procedure is required; this procedure is presented in Appendix I.

Subsequent analysis of the data has shown that there are two mechanisms of energy dissipation; both of these mechanisms contribute to the drag coefficients that were determined from Eqs. (3) and (4). For this reason, these coefficients are referred to as "apparent drag coefficients", and are denoted C_{D_*}. The second mechanism, nearly independent of "tree" spacing is related to the instability of large near-breaking waves. The hypothesis is that a small perturbation will cause a near-breaking wave in water of uniform depth to lose energy in accordance with the following equation

$$\frac{dH^2}{dx} = -\frac{K}{h}(H^2 - H_s^2) \qquad (5)$$

in which K is a damping coefficient possibly depending on beach slope and H_s is a stable wave height presumed to be proportional to water depth. Denoting the A values (Eq. (3)) associated with the apparent drag coefficients, C_{D_*}, as A_*, it follows that

$$\frac{dH}{dx} = -A_* H^2 = -AH^2 - f(x) \qquad (6)$$

which is developed in Appendix I. In Eq. (6), f(x) represents the portion of the wave decay attributable to wave instability damping as given by f(x), i.e.

$$f(x) = \frac{K}{2hH}(H^2 - H_s^2)$$

The f(x) and A values were determined from pairs of tests at different tree densities but which have the same nominal wave heights and water depths. The procedures are presented in Appendix II and the results described later. Finally the values of the wave instability coefficient, K, and the ratio of the stable wave height, H_s, to water depth, h, were determined using a least squares procedure. Again, the methodology of determining K and H_s is presented in Appendix II.

V. RESULTS OF DATA ANALYSIS

Based on an inspection of the experimentally-determined drag coefficient values presented in Tables II-IV, it is clear that the damping is much higher than could be attributed to drag coefficients determined from steady-state analysis. For example, Figure 4 presents the variation of drag coefficient versus Reynolds Number, R, for smooth circular cylinders and steady flow. It is seen that the range of drag coefficients is 0.95 to 1.2 for Reynolds Numbers over the range $600 < R < 3 \times 10^5$. For reference purposes, based on small amplitude shallow water wave theory, the maximum Reynolds number, R, is given by

$$R = \frac{\frac{H}{2}\sqrt{\frac{g}{h}}\,D}{\nu}$$

TABLE II

SUMMARY OF FULL FOREST DENSITY RESULTS

Run No.	Water Depth, h (cm)	Wave Period, T (sec)	Initial Wave Height, H_o (cm)	C_D *	ΔH (cm)	Water Temp. (^oC)
F-1	20	1.08	13.62	1.93	6.63	-
F-2	20	1.35	13.76	2.31	7.34	-
F-3	20	1.58	16.15	2.68	9.83	12.5
F-4	20	1.00	7.54	1.61	2.29	-
F-5	20	1.34	8.05	2.22	3.15	-
F-6	20	1.60	8.54	1.73	2.96	15.5
F-7	20	1.10	3.60	2.59	0.90	-
F-8	20	1.33	3.47	1.78	0.63	-
F-9	20	1.60	4.41	1.95	1.05	-
F-10	10	1.05	6.39	3.75	4.05	-
F-11	10	1.10	7.32	4.11	5.01	13.0
F-12	10	1.33	8.25	3.84	5.74	-
F-13	10	1.04	3.94	3.70	2.02	-
F-14	10	1.33	4.30	3.06	2.09	-
F-15	10	1.65	4.06	1.96	1.48	-
F-16	10	1.66	4.11	1.97	1.51	-
F-17	10	1.06	1.85	3.07	0.54	-
F-18	10	1.36	2.39	2.39	0.70	-
F-19	10	1.65	2.31	3.28	0.82	-

TABLE III

SUMMARY OF HALF FOREST DENSITY RESULTS

(δ = 10.16 cm)

Run No.	Water Depth, h (cm)	Wave Period, T (sec)	Initial Wave Height, H_o (cm)	C_{D_*}	ΔH (cm)	Water Temp. (^oC)
H-1	20	1.00	13.49	8.04	6.66	15.5
H-2	20	1.32	15.72	3.68	5.38	15.0
H-3	20	1.56	15.42	6.98	7.58	15.0
H-4	20	0.96	7.69	1.54	0.74	15.5
H-5	20	1.30	7.67	1.11	0.54	15.0
H-6	20	1.59	8.45	3.86	1.92	14.0
H-7	20	1.04	4.48	4.41	0.68	-
H-8	20	1.30	3.77	3.83	0.43	15.5
H-9	20	1.60	4.08	5.23	0.66	14.5
H-10	10	1.03	6.10	13.48	3.64	14.5
H-11	10	1.31	7.76	12.44	4.93	14.5
H-12	10	1.64	7.40	14.02	4.82	-
H-13	10	1.02	3.74	4.50	0.87	13.5
H-14	10	1.35	4.09	6.05	1.26	13.5
H-15	10	1.59	3.91	5.63	1.11	14.5
H-16	10	1.04	3.51	8.79	1.25	14.0
H-17	10	1.33	2.38	6.13	0.50	15.0
H-18	10	1.65	1.61	1.17	0.05	14.0

TABLE IV

SUMMARY OF QUARTER FOREST DENSITY RESULTS

(δ = 20.32 cm)

Run No.	Water Depth, h (cm)	Wave Period, T (sec)	Initial Wave Height, H_o (cm)	C_{D_*}	ΔH (cm)	Temp. (^oC)
Q-1	20	1.07	12.72	15.20	3.85	11
Q-2	20	1.31	15.10	23.69	6.73	11
Q-3	20	1.60	15.35	16.69	5.61	11
Q-4	20	1.03	8.65	8.22	1.19	10
Q-5	20	1.31	8.05	3.62	0.49	11
Q-6	20	1.61	6.68	20.80	1.59	11
Q-7	20	1.00	4.39	4.05	0.17	11
Q-8	20	1.29	3.48	8.07	0.21	11
Q-9	20	1.61	3.77	23.51	0.63	11
Q-10	10	1.00	6.79	39.20	3.70	16
Q-11	10	1.28	6.47	33.83	3.17	16
Q-12	10	1.60	5.66	47.76	3.11	16
Q-13	10	0.99	3.55	14.16	0.65	14.9
Q-14	10	1.29	4.08	22.42	1.19	14.5
Q-15	10	1.62	4.39	8.39	0.62	14.5
Q-16	10	0.97	2.06	22.63	0.36	14.5
Q-17	10	1.32	1.84	35.09	0.41	-
Q-18	10	1.66	1.94	14.03	0.21	15.0

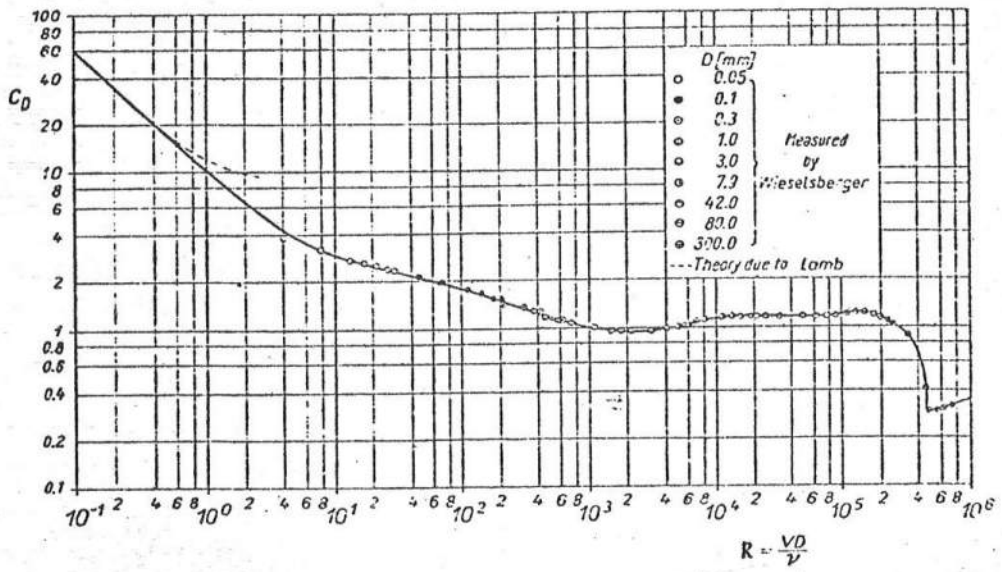

FIGURE 4. DRAG COEFFICIENT FOR A SMOOTH CIRCULAR CYLINDER IN STEADY FLOW (FROM SCHLICHTING).

in which ν is the kinematic viscosity of water. For typical values of H = 4 cm, h = 10 cm, D = 0.5 cm, g = 980 cm/s^2, $\nu = 1.1 \times 10^{-2}$ cm^2/s

$$R \cong 900$$

which from Figure 4 should ensure that these conditions would result in drag coefficients in the usual range noted above.

Nonlinear Effects

In deriving Eq. (1), linear shallow water wave theory was used and it was assumed that the effects of the water surface displacement from the mean level were small. It is known that there are substantial differences between the kinematics of nonlinear and linear wave theories and therefore, this represents a possible explanation for the large drag coefficients extracted from the measured wave height data.

The tabulations of the Stream Function wave theory (Dean (1974)) were utilized to evaluate the magnitudes of the effects of nonlinear waves. The following were chosen as reasonably representative wave conditions

$$H = 4 \text{ cm}$$

$$h = 10 \text{ cm}$$

$$T = 1.3 \text{ sec.}$$

which leads to deep water relative depth and wave steepness values of

$$h/L_o = 0.038$$

$$H/L_o = 0.0152$$

These values are reasonably well approximated by those of Case 5-B for which

$$h/L_o = 0.050$$

$$H/L_o = 0.020$$

Energy losses are related to the following integral, the values of which were compared for linear and stream function wave theories

$$\int_0^{\pi}\int_0^{S_\eta} |u'|^3 dS|d\theta \tag{9}$$

in which u' is the dimensionless horizontal velocity component, defined as

$$u' = \frac{u(S,\theta)}{H/T} \tag{10}$$

and S is a coordinate directed vertically upward from the bottom and

$$S_\eta = h + \eta \quad \text{(nonlinear case)}$$

$$S_\eta = h \quad \text{(linear case)}$$

It was found that for Case 5-B, the two integrals for the linear and nonlinear theories agreed within 18%. Although this comparison was only carried out for Case 5-B, it was concluded that nonlinear effects could not possibly account for the magnitudes of the apparent drag coefficients.

Effects of Oscillating Versus Steady Flows

As noted previously, for steady flow, the drag coefficient depends only on Reynolds Number and cylinder roughness. With the introduction of an oscillating flow, the dependence is extended to include an additional parameter which was first defined by Keulegan and Carpenter (1958) and is referred to as the "Keulegan-Carpenter" parameter, KC, or "Period Parameter" as defined by

$$KC = \frac{U_m T}{D} \qquad (11)$$

in which U_m is the maximum oscillating water particle velocity, T is the wave period and D is the cylinder diameter. Sarpkaya (1976a), (1976b), (1976c) has carried out extensive measurements of drag and inertia coefficients for a circular cylinder for wide ranges of Reynolds Numbers and period parameters. Sarpkaya has found that for low Reynolds Numbers, the drag coefficients are larger than for steady flow. The smallest Reynolds Numbers reported by Sarpkaya were approximately 10^4 and the associated drag coefficients were on the order of 2.0 (versus approximately 1.2 for steady flow). Although the Reynolds Numbers associated with the wave tank measurements of this study were less than those reported by Sarpkaya, based on considerations of the cylinder wake, it does not appear that the drag coefficient could be much greater than 2.5.

Effects of Reflected Waves

As discussed in an earlier section, there was considerable wave reflection from the down-wave end of the tank (up to 20%, but generally less than 10%). Although a detailed analysis of the associated effect has not been made, approximate considerations of the effect of reflections of the magnitude noted would not account for the drag coefficient values determined.

Effects of Instability of Waves

For waves propagating into gradually decreasing depths, the usual assumption is that the waves will shoal (increase in height) until the height is about 78% of the depth, then the wave height will continue to break to maintain the 0.78 ratio. This simple model is convenient, but unfortunately not very representative of the actual phenomenon for the situation noted. In

actuality, water waves near breaking are not very stable and, if perturbed, they will lose energy such that the stable wave height will be considerably less than 0.78 of the local depth. To fix ideas consider the case in which a wave is propagating from a gradually sloped region to a region of uniform depth and that breaking just occurs at the junction between the sloping and horizontal sections. The simple model discussed earlier would indicate that the wave height on the uniform depth segment would remain at 0.78 of the water depth. In reality, once breaking starts, energy dissipation continues and the wave height on the horizontal segment would stabilize at a value considerably less than 0.78 of the depth.

The following approach to this problem is based primarily on data collected by Horikawa and Kuo (1966) and a study in progress of these and other data as part of a Master of Science thesis by Mr. Bill Dally at the University of Delaware. Figure 5 presents wave height variations as measured by Horikawa and Kuo for a plane beach slope of 1:65. The straight line $H = 0.78\ h$ is presented on this plot and it is seen that, depending on the deep water wave steepness, the wave height initially exceeds the 0.78 line, then breaking occurs more rapidly than the depth decreases with distance and the wave height drops below the 0.78 line. It is clear that if the waves were to propagate onto a horizontal segment, the wave height would continue to decrease to some stable value. Even on a sloping beach some of the wave heights in this figure are approximately only 60% of the local depth.

Interpretation

This section presents an interpretation of the wave damping results. In general, of the possible mechanisms discussed, the data support the hypothesis of a perturbation triggering wave damping which is especially severe if the wave conditions are initially at near-breaking conditions. In the "tree" tests

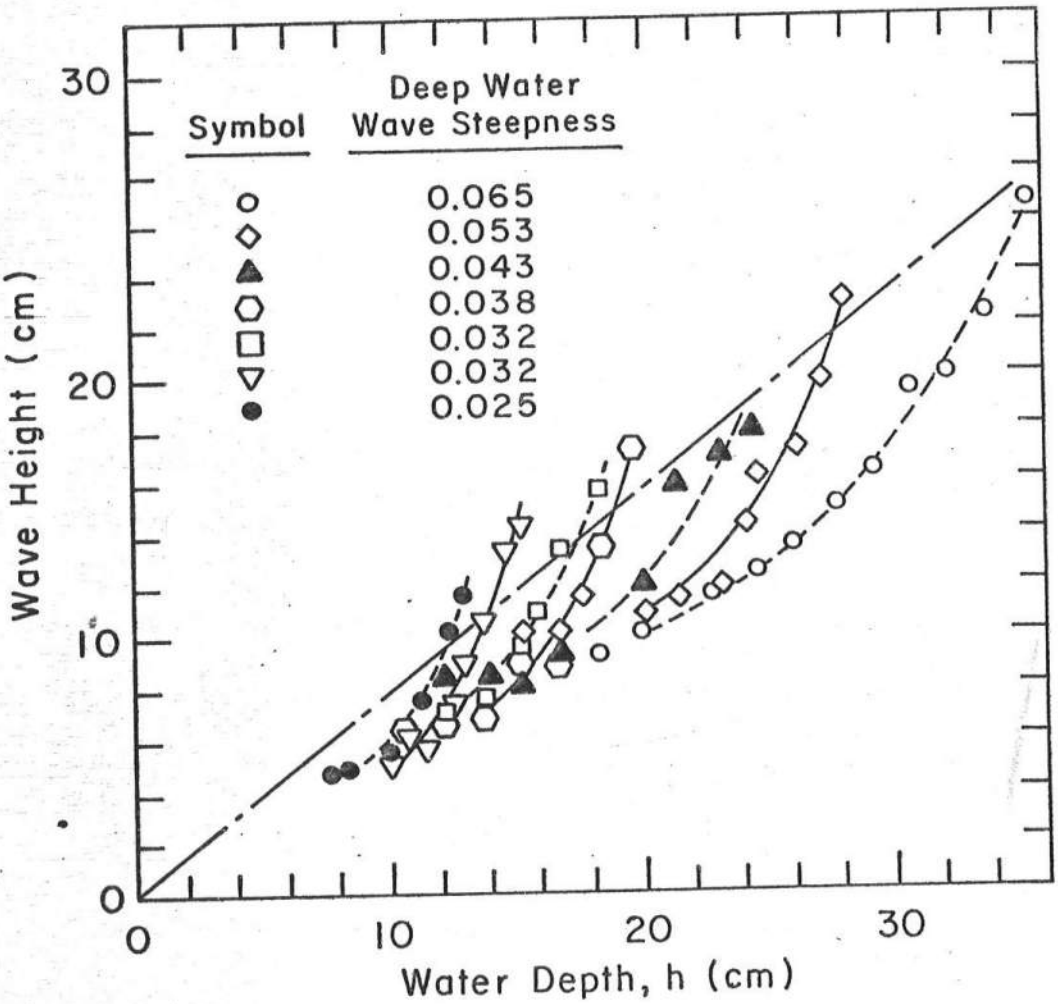

FIGURE 5. VARIATION OF WAVE HEIGHT FOLLOWING BREAKING. PLANE BEACH, SLOPE = 1:65, WAVE PERIOD, T = 1.6 SEC. (FROM HORIKAWA AND KUO).

reported here, the damping was due to the tree elements which caused direct damping through the drag forces and indirect damping through the initiation of the wave instability mechanism. Thus the overall damping is much greater than can be attributed solely to drag on the vegetation elements. The relative contribution of the instability mechanism increases with increasing tree spacing because of the decrease in the direct damping mechanism.

Numerical Results

Appendix II presents the data analysis procedures and the detailed numerical results obtained. Briefly, the results support both vegetative and wave instability damping with a reasonable value of 1.0 for the drag coefficient to represent vegetative damping and values of K and H_s/h of 0.08 and 0.30 respectively to represent wave instability damping.

VI. RECOMMENDED CALCULATION PROCEDURE

Recommendations

Based on an analysis of the wave tank tests carried out in conjunction with this project and of previous results published by Horikawa and Kuo, it is recommended that the HUD wave effect calculation procedure include contributions to wave damping due to both vegetation effects and wave instability. The recommended calculation procedure is detailed below for the case of a horizontal bottom and uniform vegetation characteristics. More comprehensive methodology could be developed for general conditions.

For simple situations in which either the vegetative or wave instability damping can be considered to act singly, analytical solutions exist for the variation of wave height with distance. For cases where the combined effects

are significant, or a sloping bottom exists, it is necessary to employ a simple numerical approach. The recommended procedures are presented below.

a) Damping Due to Vegetation, Uniform Depth

$$H(x) = \frac{1}{1 + AH_o x} \tag{12}$$

b) Damping Due to Wave Instability Effects, Uniform Depth

$$H(x) = \sqrt{H_s^2 + (H_o^2 - H_s^2)e^{-Kx/h}} \tag{13}$$

c) Damping Due to Combined Effects of Vegetation and Wave Instability Effects, Uniform Depth

$$H_{j+1} = H_j - \Delta x\left[AH_j^2 + \frac{K}{2hH_j}(H_j^2 - H_s^2)\right], \quad H_j > H_s \tag{14a}$$

$$H_{j+1} = H_j - \Delta x AH_j^2 \quad , H_j < H_s \tag{14b}$$

in which H_{j+1} and H_j represent the wave heights at x_{j+1} and x_j and $\Delta x = x_{j+1} - x_j$.

In the above equations, it is recommended that the following values be used

$$C_D = 1.0$$

$$K = 0.08$$

$$H_s/h = 0.30$$

Example Calculations

Three example calculations will be presented illustrating the application of Eqs. (12), (13) and (14).

a) Damping Due to Vegetation

Consider trees of 30 cm diameter extending through the water column and on spacings of 2 meters. A mean water depth of 3 meters is selected for this example, the recommended drag coefficient is 1.0 and the initial wave height is 2 meters.

$$A = \frac{C_D D}{3\pi\delta^2 h} = \frac{(1.0)(0.3)}{3\pi(2)^2 3} = 0.265 \times 10^{-2}\ m^{-2}$$

Employing Eq. (12),

$$H(x) = \frac{2}{1 + 0.00531\ x}$$

and the results are presented as Curve (a) in Figure 6. This example is presented for illustration purposes only as the effects of vegetation should be sufficient to initiate the wave instability effects.

b) Damping Due to Wave Instability

Consider the wave conditions as in a). There is no vegetation present, and it is assumed that the wave instability mechanism has been initiated. Employing Eq. (13)

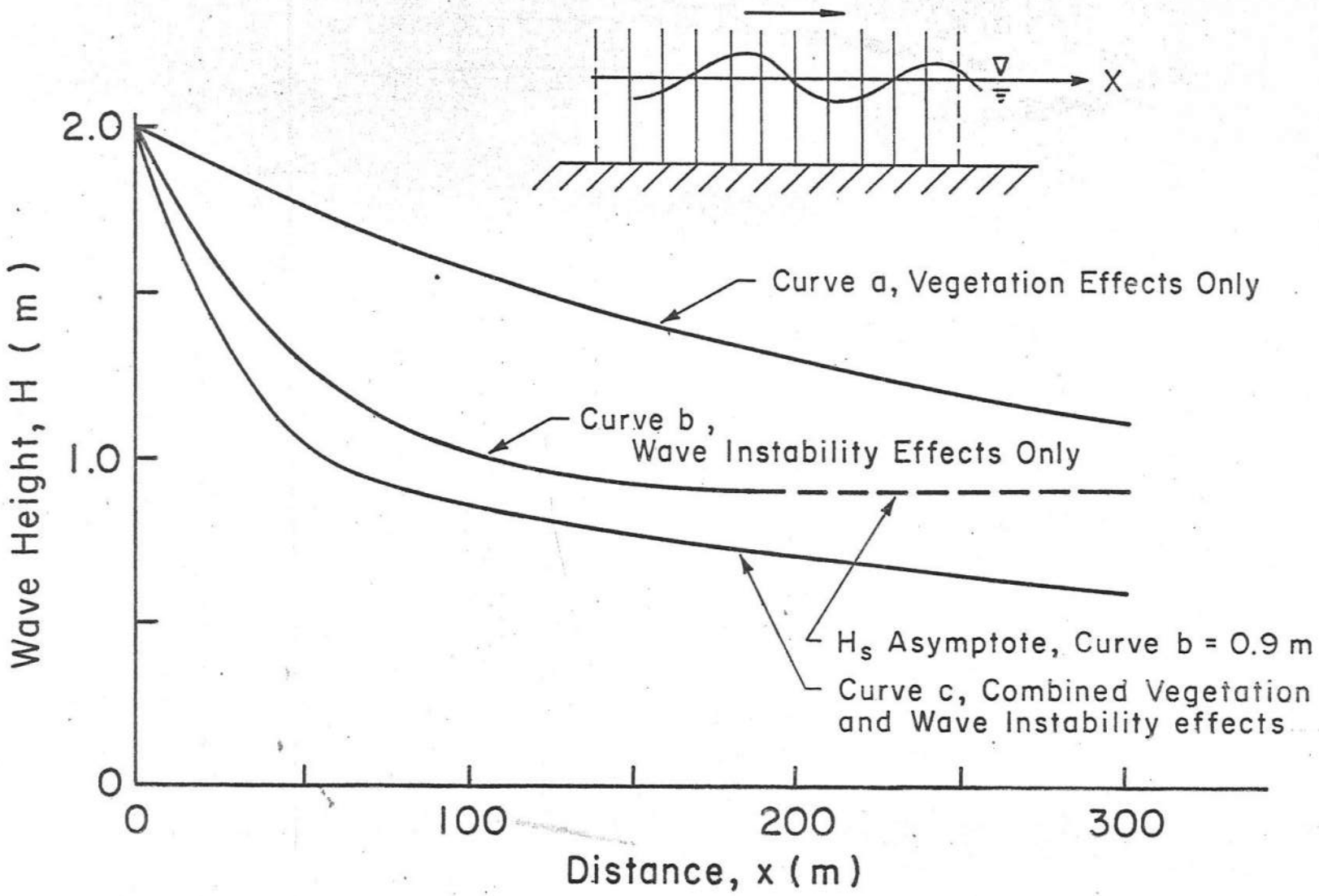

FIGURE 6. ILLUSTRATION OF WAVE DAMPING BY VARIOUS MECHANISMS

$$H(x) = \sqrt{0.81 + 3.1\, e^{-.027\, x}}$$

i.e., $H_s = 0.3\ h = 0.9$ m.

The results are presented as Curve (b) in Figure 6.

c) Damping Due to Combined Effects of Vegetation and Wave Instability

For the wave and vegetation conditions of Examples (a) and (b), Eq. (14) must be used in the form

$$H_{j+1} = H_j - 10.0\left[.265 \times 10^{-2}\, H_j^2 + \frac{0.0133}{H_j}(H_j^2 - 0.81)\right], \quad H_j > 0.9$$

$$H_{j+1} = H_j - 0.265 \times 10^{-1}\, H_j^2 \qquad , \quad H_j < 0.9$$

The results are presented in Figure 6 as Curve (c). It is noted that it is necessary to take Δx sufficiently small that the results do not depend substantially on this parameter. For this example a value of $\Delta x = 10$ m was used.

VII. SUMMARY

Based on a series of wave tank tests and consideration of available related data, a procedure has been recommended for calculating wave damping due to vegetation and wave instability effects.

VIII. REFERENCES

Dean, R. G., "Evaluation and Development of Water Wave Theories for Engineering Application", Volume I: Presentation of Research Results; Volume II: Tabulation of Dimensionless Stream Function Theory Variables," Special Report No. [illegible], Published by U. S. Army Corps of Engineers, Coastal Engineering Research Center, Fort Belvoir, Virginia, November, 1974.

Horikawa, H. and C. T. Kuo, "A Study of Wave Transformation Inside the Surf Zone", Proceedings, Tenth Conference on Coastal Engineering, Chapter 15, 1966, p. 217-233.

Keulegan, G. H. and L. H. Carpenter, "Forces on Cylinders and Plates in an Oscillating Fluid," Journal of Research of the National Bureau of Standards, Vol. 60, No. 5, p. 423-440, May 1958.

National Academy of Sciences Panel on Wave Action Effects Associated with Storm Surges, "Methodology for Calculating Wave Action Effects Associated with Storm Surges," Washington, D. C., 1977.

Sarpkaya, T., "In-Line and Transverse Forces on Cylinders in Oscillatory Flow at High Reynolds Numbers", Offshore Technology Conference, Paper No. 2533, May 1976.

Sarpkaya, T., "Vortex Shedding and Resistance in Harmonic Flow About Smooth and Rough Circular Cylinders at High Reynolds Numbers", U. S. Naval Postgraduate School, Report No. NPS-59SL76021, Feb. 1976.

Sarpkaya, T., "In-Line and Transverse Forces on Smooth and Sand-Roughened Cylinders in Oscillatory Flow at High Reynolds Numbers", U. S. Naval Postgraduate School, Report No. NPS-69SL76062, June 1976.

Schlichting, H., "Boundary-Layer Theory", McGraw-Hill Book Co., Sixth Edition, New York, 1968, p. 17.

APPENDIX I - FORMULATION OF RELATIONSHIPS FOR ANALYSIS

Wave Height Damping Due to Vegetation

Consider waves propagating through vegetation characterized by vertical cylinders of diameter, D, extending through the water column and on an average spacing, δ. Wave energy considerations yield

$$\frac{d(EC_G)}{dx} = -\mathcal{D} \tag{I-1}$$

in which E = the average wave energy per unit surface area, C_G = group velocity and $\mathcal{D}$ = average wave energy loss per unit time in a water column of unit surface area. Consideration of the drag forces, F_D, acting on a vegetative element yields the average energy loss rate, $\bar{\dot{e}}$, associated with that element as

$$\bar{\dot{e}} = \overline{F_D u} \tag{I-2}$$

in which

$$F_D = \int_0^{h+\eta} \frac{C_D \rho D}{2} u|u| ds \tag{I-3}$$

In Eq. (I-3), C_D = drag coefficient (of order unity), h = mean water depth and η = instantaneous water surface displacement. In the following, shallow water will be considered and it will also be assumed that for purposes here, it is possible to replace $\eta + h$ by h in Eq. (I-3). The horizontal water particle velocity, u, as given by shallow water linear wave theory is

$$u = \frac{H}{2}\sqrt{\frac{g}{h}} \cos \sigma t \tag{I-4}$$

The wave energy, E, and shallow water group velocity are given by

$$E = \rho g \frac{H^2}{8}$$

$$C_G = \sqrt{gh} \qquad \text{(I-5)}$$

Substituting Eqs. (I-2), (I-3), (I-4) and (I-5) into (I-1), the following results for uniform depth

$$\frac{dH}{dx} = - \frac{C_D D H^2}{3\pi\delta^2 h} = -AH^2 \qquad \text{(I-6)}$$

Damping Due to Wave Instability

Inspection of data collected in this program and by Horikawa and Kuo (1966) has resulted in the hypothesis that for waves with fairly near-breaking heights, a small perturbation will induce breaking which will then continue to a state where the wave height reaches some stable wave height, H_s. Based, in part, on a study in progress by Mr. Bill Dally at the University of Delaware, the following equation has been selected for representing the wave height decay

$$\frac{dH^2}{dx} = - \frac{K}{h}(H^2 - H_s^2) \qquad \text{(I-7)}$$

which states that the rate of energy loss is proportional to the "excess" of wave energy. In Eq. (I-7), K is termed a wave instability damping coefficient, which varies with beach slope. The data by Horikawa and Kuo show that K increases with beach slope. It can be shown that for uniform depth conditions, the solution to Eq. (I-7) is

$$H(x) = \sqrt{H_s^2 + (H_o^2 - H_s^2)e^{-Kx/h}} \qquad \text{(I-8)}$$

Damping Due to Combined Effects of Vegetation and Wave Instability

In the absence of data to the contrary, it is reasonable to assume that the damping due to combined effects of vegetation and wave instability can be superimposed, i.e.

$$\frac{dH}{dx} = -A_* H^2 = -AH^2 - f(x) \qquad \text{(I-9)}$$

in which A_* is based on the measured wave heights and hence includes both effects, and f(x) is due to wave instability damping and is determined from Eq. (I-7) as

$$f(x) = \frac{K}{2hH}(H^2 - H_s^2) \qquad \text{(I-10)}$$

APPENDIX II - DETERMINATION OF DRAG COEFFICIENTS AND ENERGY DAMPING CHARACTERISTICS

Introduction

This appendix describes the detailed methodology employed to analyze the data. First, the method is presented of extracting the apparent drag coefficients, C_{D_*}, and initial wave heights, H_o, from the data using a nonlinear least squares procedure. Secondly, a description is presented of the combination of pairs of averages of data groups to determine C_D and f(x) values. Finally using the f(x) results, a linear least squares procedure is developed to determine the wave instability damping coefficient, K, and the ratio of stable wave height, H_s, to water depth, h.

Determination of Apparent Drag Coefficient, C_{D_*}, and Initial Wave Height, H_o

The wave tank studies resulted in the variation of measured wave height with distance for various water depths, initial wave heights and "forest" densities represented by arrays of dowels. The characteristics of these tests have been described in Section II of this report. The theory developed in Appendix I has resulted in the following variation of predicted wave height, H_p, with distance, x,

$$H_p(x) = \frac{H_o}{1 + AH_o x} \qquad \text{(II-1)}$$

in which H_o is the wave height at x = 0 and, the drag coefficient, C_D, is defined in terms of A as

$$C_D = \left(\frac{3\pi\delta^2 h}{D}\right)A \qquad \text{(II-2)}$$

in which δ is the average center-to-center spacing of the individual dowels in the forest, h is the mean water depth, and D is the diameter of the dowels. Based on the resulting drag coefficients and investigations conducted by Horikawa and Kuo (1966), it is hypothesized that, in addition to wave damping by the dowels, additional damping occurs due to wave instability. For this reason, the resulting coefficients are denoted A_* and C_{D_*} in recognition of the effects of the wave instability damping. The purpose of this section of the appendix is to describe the method that was employed to determine the apparent drag coefficient, C_{D_*}, such that a "best fit" resulted between the measured wave height data and Eq. (II-1). The method used was to determine the unknowns, H_o and A_*, so as to minimize the sum of the squares of the deviations between the measured and predicted wave heights.

Denote ε_i as the difference between the i^{th} measured and predicted wave height, i.e.

$$\varepsilon_i \equiv H_{p_i} - H_{m_i} \tag{II-3}$$

The objective is to determine H_o and A_* such that the following is minimized

$$\sum \varepsilon_i^2 = \sum \left(H_{p_i} - H_{m_i}\right)^2 \tag{II-4}$$

If the equation relating H_{p_i} to the unknowns, H_o and A_*, were linear in these unknowns, it would be possible to use the usual least-squares procedure. However, in this case it is necessary to employ a nonlinear least-squares procedure. Expanding H_{p_i} in a first-order Taylor's series in A_* and H_o

$$H_{p_i}^{j+1} = H_{p_i}^{j} + \frac{\partial H_{p_i}}{\partial H_o} \Delta H_o + \frac{\partial H_{p_i}}{\partial A_*} \Delta A_* \qquad \text{(II-5)}$$

where the superscripts denote the iteration number and indicate that the predicted wave height at the i^{th} location at the $(j + 1)^{th}$ iteration will be modified due to changes in the two unknowns, H_o and A_*. An iterative procedure is used to determine H_o and A_*.

Inserting Eq. (II-5) into (II-4),

$$\sum \varepsilon_i^2 = \sum \left(H_{p_i} + \frac{\partial H_{p_i}}{\partial H_o} \Delta H_o + \frac{\partial H_{p_i}}{\partial A_*} \Delta A_* - H_{m_i} \right)^2 \qquad \text{(II-6)}$$

and ΔH_o and ΔA_* are found by the usual least squares procedures

$$\left.\begin{aligned} \frac{\partial \sum \varepsilon_i^2}{\partial (\Delta H_o)} &= 0 \\ \frac{\partial \sum \varepsilon_i^2}{\partial (\Delta A_*)} &= 0 \end{aligned}\right\} \qquad \text{(II-7)}$$

These two equations, when expanded yield the following two simultaneous equations for the two unknowns, ΔH_o and ΔA_*,

$$\left.\begin{aligned} \Delta H_o S_1 + \Delta A_* S_2 &= S_3 \\ \Delta H_o S_2 + \Delta A_* S_4 &= S_5 \end{aligned}\right\} \qquad \text{(II-8)}$$

where

$$
\left.
\begin{aligned}
S_1 &= \sum \left(\frac{\partial H_{p_i}}{\partial H_o}\right)^2 \\
S_2 &= \sum \left(\frac{\partial H_{p_i}}{\partial H_o}\right)\left(\frac{\partial H_{p_i}}{\partial A_*}\right) \\
S_3 &= \sum \left(H_{m_i} - H_{p_i}\right)\left(\frac{\partial H_{p_i}}{\partial H_o}\right) \\
S_4 &= \sum \left(\frac{\partial H_{p_i}}{\partial A_*}\right)^2 \\
S_5 &= \sum \left(H_{m_i} - H_{p_i}\right)\left(\frac{\partial H_{p_i}}{\partial A_*}\right)
\end{aligned}
\right\} \qquad \text{(II-9)}
$$

and the summation extends over the wave heights at all x values. The solution of Eq. (II-8) is

$$
\left.
\begin{aligned}
\Delta H_o &= \frac{S_3 S_4 - S_2 S_5}{S_1 S_4 - S_2^2} \\
\Delta A_* &= \frac{S_1 S_5 - S_2 S_3}{S_1 S_4 - S_2^2}
\end{aligned}
\right\} \qquad \text{(II-10)}
$$

The revised (improved) values of H_o and A_* are determined as

$$
\left.
\begin{aligned}
H_o^{j+1} &= H_o^j + \Delta H_o \\
A_*^{j+1} &= A_*^j + \Delta A_*
\end{aligned}
\right\} \qquad \text{(II-11)}
$$

This process is repeated until the changes ΔH_o and ΔA_* are small. In the calculations here, eight iterations were routinely used; however the results had usually stabilized after three iterations.

Example - Figure 3 has presented an example of experimental data for Run No. F-3 and the fit provided to that data. Figure II-1 shows the coefficients H_o and A_* for Run No. F-3 and the variation of root-mean-square error $\sqrt{\varepsilon_i^2}$ with iteration.

Separation of Drag Coefficient and Wave Instability Damping

Although the total wave damping is relevant to the situation of wave propagation across a particular vegetated profile, it is of interest to this study to separate the two effects to better quantify their individual contributions and to provide a better basis for calculation. In particular the effective drag coefficients, C_{D_*}, determined in the preceding section are large due to including an as yet unquantified effect due to wave instability. The following analysis is based on the reasonable premise that (1) the wave instability damping will be the same for different "tree" densities if the wave heights are approximately the same, and (2) the form of the relationship for wave height damping (Eq. (II-1)) provides a reasonable fit to the data even if there is a substantial amount of wave instability damping present.

The total wave damping can be expressed as

$$\frac{dH}{dx} = -\frac{1}{3\pi}\frac{C_{D_*} D}{\delta^2 h} H^2 \qquad \text{(II-12)}$$

and for purposes here, we will denote

$$A_* = \frac{1}{3\pi}\frac{C_{D_*} D}{\delta^2 h} \qquad \text{(II-13)}$$

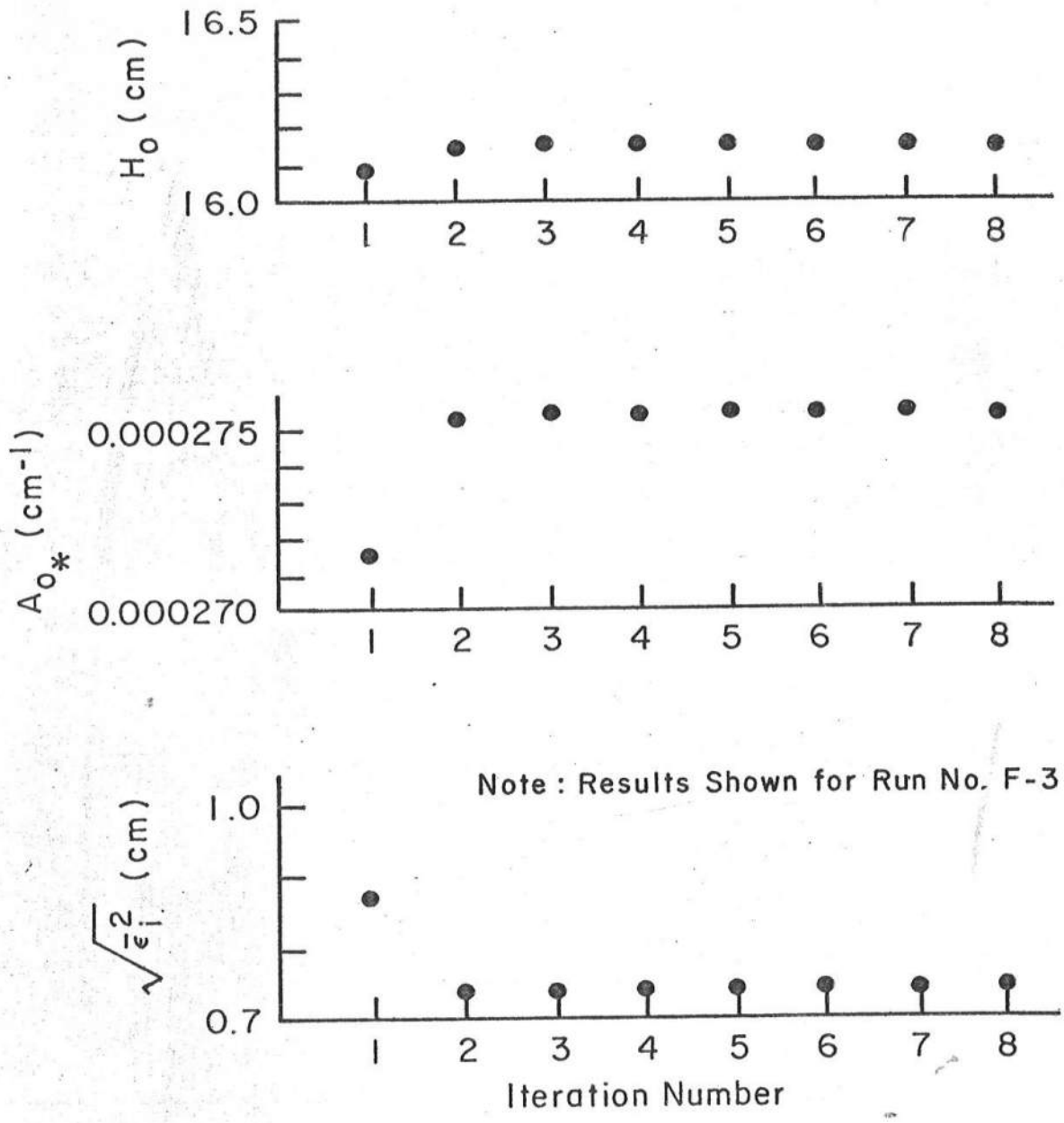

FIGURE II-1. STABILIZATION OF INITIAL WAVE HEIGHT, H_o, DAMPING COEFFICIENT, A_*, AND ROOT-MEAN SQUARE ERROR, $\sqrt{\bar{\epsilon}_i^2}$ WITH ITERATION NUMBER.

The total damping will be separated into a contribution due to drag on the dowels given by an expression similar to Eq. (II-12) with the actual drag coefficient, C_D, replacing the effective drag coefficient, C_{D_*}, and an unspecified form of wave instability damping denoted here as f(x),

$$\frac{dH}{dx} = -A_* H^2 = -\frac{G}{\delta^2} H^2 - f(x) \qquad \text{(II-13)}$$

in which G is defined as

$$G = \frac{C_D D}{3\pi h} \qquad \text{(II-14)}$$

Expressing Eq. (II-13) for two different forest densities and approximately the same wave height, the value of G is determined from the associated values of A_* by solving this set of simultaneous equations

$$G = \frac{\delta_1^2 \delta_2^2}{\delta_2^2 - \delta_1^2}\left(A_{*_1} - A_{*_2}\right) \qquad \text{(II-15)}$$

which, as expected, is independent of wave height. The value of C_D can be determined from Eq. (II-14),

$$C_D = \frac{3\pi h G}{D} \qquad \text{(II-16)}$$

The wave energy damping values are determined as

$$f(x) = \left(\frac{\delta_1^2 \delta_2^2}{\delta_1^2 - \delta_2^2}\right)\left(\frac{A_{1_*}}{\delta_2^2} - \frac{A_{2_*}}{\delta_1^2}\right) H^2 \qquad \text{(II-17)}$$

Drag coefficients calculated in this manner are in much better agreement with those generally used in engineering practice both in unidirectional and oscillating flows. Eqs. (II-15) and (II-17) are applied by first averaging the A_* values for the tests with a common tree spacing and nearly-common wave height, then applying Eqs. (II-15), (II-16) and (II-17). The averaged A_* and C_{D_*} values are presented in Table II-1. Table II-2 presents the $f(x)$ and C_D values determined from the data of various test groups.

Although the drag coefficients presented in Table II-2 are much more reasonable than those in Tables II, III and IV, due to the removal of the wave instability damping effects, they are still considerably larger than the normal values ($\approx$1.2) associated with unidirectional flows or those ($\approx$2.0) associated with oscillatory flows for the ranges of Reynolds Numbers and period parameters in these tests. The reasons for these high drag coefficients are believed to be due to: (1) the relatively low drag-related damping especially for the one-quarter density tests and the data therefore not being well-conditioned for determining the drag coefficients, and (2) possibly the Reynolds Number being lower in the tests than would occur under natural conditions. For these reasons, a drag coefficient of unity will be recommended in the calculation procedure.

TABLE II-1

SUMMARY OF RESULTS AVERAGED BY WAVE HEIGHT GROUP

a) Full Forest Density

$\overline{H_o}$ (cm)	h (cm)	$\overline{C_{D_*}}$	$\overline{A_*}$ (cm^{-1})	No. of Tests, N
14.51	20	2.31	2.279×10^{-4}	3
8.04	20	1.85	1.826×10^{-4}	3
3.83	20	2.11	2.082×10^{-4}	3
7.32	10	3.90	7.697×10^{-4}	3
4.10	10	2.67	5.269×10^{-4}	4
2.18	10	2.91	5.743×10^{-4}	3

b) Half Forest Density

$\overline{H_o}$ (cm)	h (cm)	C_{D_*}	$\overline{A_*}$ (cm^{-1})	No. of Tests, N
14.88	20	6.23	1.537×10^{-4}	3
7.94	20	2.17	0.535×10^{-4}	3
4.11	20	4.49	1.108×10^{-4}	3
7.09	10	13.31	0.657×10^{-4}	3
3.91	10	5.39	2.659×10^{-4}	3
2.50	10	5.36	2.645×10^{-4}	3

TABLE II-I
(Continued)

SUMMARY OF RESULTS AVERAGED BY WAVE HEIGHT GROUP

c) Quarter Forest Density

$\overline{H}_o$ (cm)	h (cm)	$\overline{C}_{D_*}$	$\overline{A}_*$ (cm^{-1})	No. of Tests, N
14.39	20	18.53	1.142×10^{-4}	3
7.79	20	10.88	0.671×10^{-4}	3
3.88	20	11.88	0.733×10^{-4}	3
6.31	10	40.26	2.48×10^{-4}	3
4.01	10	14.99	0.924×10^{-4}	3
1.95	10	23.92	0.148×10^{-4}	3

TABLE II-2

SUMMARY OF f(x), C_D and $\sqrt{\overline{H^2}}$ VALUES

ASSOCIATED WITH VARIOUS TEST PAIRS

a) Based on Full and Half Density Forests

Wave Height Range	Depth (h) (cm)	$\sqrt{\overline{H^2}}$ (cm)	C_D	f(x)
Large	20	14.70	1.98	0.028
Medium	20	7.99	3.43	0.000711
Low	20	3.97	2.59	0.00124
Large	10	7.21	1.50	0.0322
Medium	10	4.01	3.47	0.0029
Low	10	2.35	4.12	0.000896

b) Based on Full and Quarter Density Forests

Wave Height Range	Depth, h (cm)	$\sqrt{\overline{H^2}}$ (cm)	C_D	f(x)
Large	20	14.45	2.46	0.0223
Medium	20	7.92	2.50	0.0037
Low	20	3.86	2.92	0.001
Large	10	6.83	5.64	0.0100
Medium	10	5.77	5.02	0.000517
Low	10	2.07	4.61	0.000509

TABLE II-2
(Continued)

SUMMARY OF $\sqrt{\overline{H^2}}$, C_D and f(x) VALUES

ASSOCIATED WITH VARIOUS TEST PAIRS

c) Based on Half and Quarter Density Forests

Wave Height Range	Depth (h) (cm)	$\sqrt{\overline{H^2}}$ (cm)	C_D	f(x)
Large	20	14.64	4.27	0.0216
Medium	20	7.87	-1.47	0.0044
Small	20	4.00	4.05	0.0010
Large	10	6.71	22.09	0.0050
Medium	10	3.96	9.38	0.000542
Small	10	2.24	6.32	0.000538

Determination of K and H_s/h

The f(x) values reported in Table II-2 were utilized to determine estimates of K and H_s/h in the following equation

$$\frac{\partial H^2}{\partial x} = -\frac{K}{h}(H^2 - H_s^2) \qquad \text{(II-18)}$$

in which H_s represents a "stable" or equilibrium wave height and K represents a wave instability damping coefficient. A least squares procedure was employed in which the governing equations were Eq. (II-18) and the following

$$\frac{dH}{dx} = -A_* H^2 = -AH^2 - f(x) \qquad \text{(II-19)}$$

in which A_* is related to the apparent drag coefficient C_{D_*} in the form of Eq. (II-12) and f(x) is determined from Eq. (I-10) as

$$f(x) = \frac{K}{2hH}(H^2 - H_s^2) \qquad \text{(II-20)}$$

i.e., the portion of the wave height decay attributable to wave instability damping is represented by f(x) and where K should depend only on beach slope and H_s should depend primarily on water depth and possibly beach slope. As shown in Table II-2 there are nine values of f(x) available for each water depth. Using H_o as the representative value of H, and denoting each test by subscript "n", Eq. (II-20) can be rewritten in a form convenient for the least squares procedure

$$H_s^2 + \frac{f_n(x)\,2hH_n}{K} = H_n^2 \qquad \text{(II-21)}$$

The least squares procedure yields the following two equations for H_s^2 and K

$$H_s^2 = \frac{S_2 S_3 - S_1 S_4}{N S_3 - S_1^2} \qquad \text{(II-22)}$$

$$K = 2h \left[\frac{N S_3 - S_1^2}{N S_4 - S_1 S_2} \right] \qquad \text{(II-23)}$$

in which

$$S_1 = \sum_{n=1}^{N} f_n H_n$$

$$S_2 = \sum_{n=1}^{N} H_n^2$$

$$S_3 = \sum_{n=1}^{N} f_n^2 H_n^2$$

$$S_4 = \sum_{n=1}^{N} f_n H_n^3$$

and N (=9) is the total number of cases available for analysis.

The resulting values of H_s/h and K are presented in Table II-3 for depths of 10 and 20 cm.

TABLE II-3

WAVE INSTABILITY DAMPING CHARACTERISTICS FOR UNIFORM DEPTH

Water Depth (cm)	K	H_s/h
10	0.111	0.421
20	0.079	0.288

The values of K and H_s/h are considered to be in reasonably close correspondence. It is noted that the character of the pairs of H_s/h and K are somewhat compensating in that a smaller value of K and a smaller value of H_s/h would tend to result in the same variation of wave height as a larger value of K and a larger value of H_s/h. To obtain a single pair of these values, by combining all wave data, Eq. (II-21) was modified slightly to

$$h_n^2\left(\frac{H_s}{h_n}\right)^2 + \frac{2f_n(x)h_n H_n}{K} = H_n^2$$

and the results are

$$\frac{H_s}{h} = 0.2992$$

$$K = 0.0801$$

It is noted that these values are in better agreement with those developed from the 20 cm depth data than from the 10 cm data. The reason for this is probably due to the larger wave heights being associated with the 20 cm data and hence these results dominate the least squares procedure. The values recommended for application are

$$\frac{H_s}{h} = 0.30$$

$$K = 0.08$$